buildings

MDPI

Article

Environmental Impact of Earthquake-Resistant Design: A Sustainable Approach to Structural Response in High Seismic Risk Regions

Alvaro Bohorquez [1], Esteban Viteri [1], Edgar Rivera [2] and Carlos Avila [2,*]

[1] Facultad de Ingeniería Civil y Ambiental, Escuela Politécnica Nacional, Quito 170143, Ecuador; alvaro.bohorquez@epn.edu.ec (A.B.); esteban.viteri@epn.edu.ec (E.V.)
[2] Grupo de Investigación de Energía, Minas y Agua (GIEMA), Facultad de Ciencias, Ingeniería y Construcción, Universidad UTE, Quito 170527, Ecuador; edgar.rivera@ute.edu.ec
* Correspondence: carlos.avila@ute.edu.ec; Tel.: +593-999261838

Abstract: This study evaluates the environmental impact of earthquake-resistant structural design choices in high-risk seismic regions through life cycle assessment. As climate change concerns intensify, understanding the environmental implications of structural design decisions becomes crucial for sustainable construction. Examining a building in Quito, Ecuador, the research compares three structural systems: Optimized Framed System (OFS), Optimized Dual System (ODS), and Equivalent Framed System (EFS). The assessment quantifies emissions through a 'cradle to gate' approach, encompassing materials fabrication, transportation, and construction processes. The results demonstrate that the ODS achieves optimal seismic performance equal to the EFS while reducing emissions by 38%, with only 5% higher emissions than the OFS. The findings establish that effective earthquake-resistant design can simultaneously achieve structural resilience and environmental sustainability, providing valuable insights for sustainable structural engineering practices in seismic regions.

Keywords: earthquake-resistant design; environmental impact; life cycle assessment; sustainable buildings; story drift

check for updates

Citation: Bohorquez, A.; Viteri, E.; Rivera, E.; Avila, C. Environmental Impact of Earthquake-Resistant Design: A Sustainable Approach to Structural Response in High Seismic Risk Regions. *Buildings* **2024**, *14*, 3821. https://doi.org/10.3390/buildings14123821

Academic Editor: Marco Di Ludovico

Received: 16 October 2024
Revised: 14 November 2024
Accepted: 19 November 2024
Published: 28 November 2024

Copyright: © 2024 by the authors. Licensee MDPI, Basel, Switzerland. This article is an open access article distributed under the terms and conditions of the Creative Commons Attribution (CC BY) license (https://creativecommons.org/licenses/by/4.0/).

1. Introduction

The catastrophic impact of recent earthquakes underscores the urgent need for resilient construction practices in seismically active regions. Notably, the February 2023 earthquakes in Türkiye, with magnitudes of Mw 7.7 and Mw 7.6, devastated urban infrastructure across 11 cities, resulting in over 50,000 fatalities, displacing approximately 1.5 million people, and highlighting critical structural vulnerabilities in reinforced concrete (RC) buildings [1,2]. In regions like Adıyaman, inadequate reinforcement, poor concrete quality, and non-ductile detailing led to widespread structural failures, revealing deficiencies in design standards [1]. These events echo similar vulnerabilities observed in the 2016 Mw 7.8 earthquake in Ecuador, where tectonic activity along the Nazca and South American plates frequently produces powerful seismic events [3]. The Pedernales earthquake, in particular, inflicted severe damage, impacting over 6000 buildings in Portoviejo alone, emphasizing the need for robust seismic codes and resilient building practices to protect communities in this dynamic tectonic setting [3,4].

These devastating earthquakes illustrate the pressing need to address not only structural resilience, but also the significant environmental impacts associated with seismic damage and post-event repairs. Seismic events significantly impact the environment, with studies revealing substantial emissions linked to earthquake-induced damages and repairs. For instance, the 2010/2011 Canterbury Earthquake Sequence in New Zealand led to extensive building demolitions, generating millions of tons of debris and high embodied CO_2

costs, highlighting the need for resilient designs that minimize post-earthquake waste [5]. Damage to critical infrastructure, such as seaports, also increases environmental burdens, as prolonged recovery efforts drive up indirect emissions [6]. Repair-induced CO_2 emissions rise with seismic intensity, particularly in green-roof buildings that require additional materials, surpassing emissions from non-green structures [7]. Additionally, buildings with "Stronger Stiffer" designs reduce repair-related greenhouse gas contributions, which can otherwise represent up to 9% of the initial construction impact [8].

In high seismic risk regions, understanding the vulnerability of existing structures, particularly reinforced concrete buildings, is essential for developing strategies to reduce structural risk and enhance resilience. Many buildings in these areas, often constructed before modern seismic codes were established, lack sufficient ductility and are prone to significant damage or collapse during earthquakes, which underscores the need for systematic vulnerability assessments and informed decisions on retrofitting or controlled demolition and reconstruction [9]. Silva et al. (2019) [9] introduces an analytical-mechanical approach for generating seismic fragility curves that assess the structural resilience of entire urban compartments rather than single representative buildings. This urban-scale methodology integrates a diverse set of structural characteristics, such as building age, height, and architectural variations, reflecting the typological diversity of RC structures in seismic zones [9,10]. Other studies have highlighted the importance of large-scale vulnerability assessments, which draw on empirical damage data from over 25,000 RC buildings affected by earthquakes in Italy over the past fifty years to address limitations in earlier approaches that often relied on simplified models or single-building representations. These studies [9,11] reveal the high variability in collapse probability among non-ductile RC frames, especially in older buildings, due to differences in structural designs, seismic zones, and outdated construction codes, thereby providing critical insights into structural fragility and guiding targeted seismic risk mitigation strategies [10,11].

Recognizing the vulnerability of existing structures in seismic-prone regions highlights the necessity of advancing not only structural resilience but also sustainable construction practices, as the environmental footprint of the construction industry significantly contributes to global carbon emissions and resource consumption. The construction industry, as one of the largest global sectors, has a substantial impact on environmental sustainability due to its intensive resource use and carbon footprint. Global greenhouse gas emissions have been escalating annually, exacerbated by unchecked economic growth and industrialization, which in turn drive a climate crisis with widespread repercussions [12]. These emissions originate across multiple sectors, with energy production contributing 73.2% of global greenhouse gasses, followed by agriculture, forestry, and land use at 18.4%, waste at 3.2%, and industry at 5.2% [13,14]. Within this energy scope, buildings rank as one of the most significant contributors to pollution, driven by substantial energy consumption. The construction sector alone accounts for approximately 40% of annual carbon emissions [15] and consumes over 35% of global energy resources while utilizing nearly 50% of natural resources [16]. Consequently, the construction field's sustainability remains poor, with significant negative implications for environmental health.

Given these severe environmental impacts, research has focused on understanding how buildings contribute to greenhouse gas emissions, particularly in multi-story structures. Early studies [12,17–19] have highlighted the carbon footprint of buildings, often emphasizing material selection as a primary factor but omitting detailed analysis on the consumption rates of CO_2 emissions or energy use across the building lifecycle. For example, while Kim et al. (2013) [12] found lower CO_2 emissions associated with reinforced concrete buildings compared to structural steel alternatives, Cole (1998) [17] presented contrasting findings, showing reduced emissions in steel-based structures when considering both energy and CO_2 consumption.

The environmental impact of construction materials and systems has become a critical focal point in the push toward more sustainable building practices. Structural components, particularly slabs, beams, and lateral loading systems, have been identified as significant

contributors to the carbon footprint of buildings [12,17,20]. While past studies have provided insights into emissions associated with specific materials, there remains a limited understanding of how construction configurations—including the number of floors, structural systems, and span length—influence overall environmental performance. Research has shown, for example, that voided slabs emit fewer pollutants than traditional slabs during construction [21] and that steel structures generate substantial environmental impacts throughout both construction and demolition phases [20]. Furthermore, larger spans, which necessitate thicker beams and columns, are known to significantly increase environmental impact, while shorter spans have proven more efficient in reducing emissions [22].

Regional studies have provided additional insights, revealing the influence of local materials and construction techniques on environmental outcomes. In Mexico, buildings employing solid concrete ceilings and aluminum-framed windows exhibited a larger carbon footprint compared to structures using ceramic walls, vaulted ceilings, and PVC-based windows [23]. Similarly, in Peru, construction activities have been shown to account for the largest portion of CO_2 emissions, overshadowing emissions from material transportation [24]. Such findings suggest that environmental impacts vary not only by material but also by construction practices and regional contexts, highlighting the complexity of sustainability assessments in the construction industry.

Recent studies underscore that slabs and beams dominate greenhouse gas emissions, contributing between 73 and 88% of total emissions depending on material and span configurations [22]. Additionally, while prefabrication offers some potential for emission reductions through efficient material use, this benefit may be counterbalanced by increased transportation emissions. Specifically, prefabricated systems often involve larger, bulkier components that require more trips and greater fuel consumption, leading to elevated transportation emissions [25]. Consequently, the embodied carbon emissions inherent to structural systems remain a pivotal consideration in a building's lifecycle impact, influenced significantly by the choice of materials and construction methodologies.

Recent research has highlighted the potential of waste materials, such as coal bottom ash (BA) and granulated glass, to improve the environmental impact and structural properties of reinforced concrete structures. Studies have found that incorporating coal bottom ash as a partial aggregate replacement in concrete can significantly reduce construction costs and enhance mechanical properties without compromising integrity. Dash and Patro (2018) [26] demonstrated that concrete mixes containing BA exhibit improved crack resistance and flexural performance, making BA a viable alternative for cost-effective and sustainable construction. Similarly, granulated glass has been investigated for its ability to improve both compressive strength and seismic resistance in tall RC structures. For example, Karalar and Çavuşli (2022) [27] analyzed a 31-story RC structure using 3D modeling and experimental tests, showing that a 15% replacement of traditional aggregates with granulated glass increased seismic resilience, reduced displacements, and enhanced overall structural performance during seismic events.

Despite considerable advancements in reducing the carbon footprint within the construction sector, further research remains essential to develop systems that effectively minimize carbon emissions while enhancing energy efficiency. This need is particularly pronounced in developing countries, where information on the carbon footprint and sustainability of buildings is often limited. In Ecuador, for instance, preliminary studies have addressed this gap; Vázquez et al. [28] conducted a pioneering investigation into the energy consumption and CO_2 emissions associated with ready-mix concrete production. Additionally, Narvaez and Maldonado [29] evaluated a building in Ecuador, revealing that architectural design significantly influences CO_2 emissions in built structures. This study contributes to these foundational efforts by examining the use of waste materials in reinforced concrete structures, advancing knowledge on sustainable construction practices and their environmental impact.

Building on these early investigations, this study undertakes a detailed analysis of typical structural designs in Ecuador, addressing both seismic resilience and environmental

sustainability. In seismic regions, structural design requires a delicate balance between mitigating seismic forces and minimizing environmental impact. While the primary focus is often on structural resilience—specifically evaluating lateral loads, material choices, and structural dimensions—environmental assessments, such as life cycle assessment (LCA), are less common but equally crucial. This study innovatively bridges this gap by integrating LCA with seismic performance analysis to provide a holistic evaluation of structural sustainability. It uniquely emphasizes three key stages: manufacturing, transportation, and construction. By concentrating on these phases, the research highlights the environmental implications of each step within the context of common structural designs in Ecuador, thereby establishing an essential link between seismic resilience and sustainability metrics. This comprehensive approach aims to support more informed decisions in structural engineering for developing regions with high seismic activity, contributing valuable insights into sustainable structural design.

2. Materials and Methods

The methodology of this study outlines a comprehensive analysis of structural design and environmental impacts for a mid-rise building in Quito, Ecuador, located within the seismically active La Carolina area (Figure 1). This case study building, a 7-story structure with three additional basement levels, exemplifies the typical mid-altitude constructions in Quito, where municipal standards restrict building heights and mandate seismic-resilient designs due to frequent tectonic activity between the Nazca and South American plates. This section describes the selection, design, and assessment of three structural systems—the Optimized Frame System, Optimized Dual System, and an Equivalent Frame System—which were chosen to meet Ecuadorian construction standards (Supplementary Materials). Each system was evaluated for seismic resilience, lateral load behavior, and environmental footprint, using Ecuadorian codes for load and material parameters. Additionally, a life cycle assessment was conducted to measure carbon emissions and energy consumption across the systems, thereby providing insight into both structural and environmental performance in a high-seismic context.

2.1. Case Study Building

The case study focuses on a 7-story building located in the La Carolina area, a central district within Quito, Ecuador, known for its high seismic activity due to the tectonic interaction between the Nazca Plate and the South American plate. This region experiences enhanced seismic effects due to its proximity to the Carnegie Ridge, making structural resilience a priority in local construction practices [30,31]. The selection of a 7-story building is grounded in a statistical analysis conducted by the authors, examining the prevalence of mid-rise buildings in the La Carolina area. This area aligns with Quito's Land Use and Management Plan (Building Code A122), which restricts building heights to a maximum of 48 m, or approximately 12 floors [32]. As a result, a 7-story structure serves as a representative choice, capturing the typical mid-altitude construction observed in this region (Table 1). The building's latitude and longitude coordinates (-0.178332° and -78.436299°) specify its exact location within the city, allowing for precise seismic and environmental considerations. Its vertical dimensions were calculated as 18.55 m for the height without basements and 26.50 m with the inclusion of three underground levels, with each floor measuring approximately 2.65 m. The primary floor area is 255.43 m^2, resulting in a cumulative total floor area of 4150.1 m^2, in alignment with the statistical assessment conducted on buildings within this zone. For foundational stability, the site's bearing capacity was established at 0.18 MPa, determined from an in-depth geotechnical analysis specific to this location, which is characterized by type D soil, as classified in local soil engineering standards [33,34].

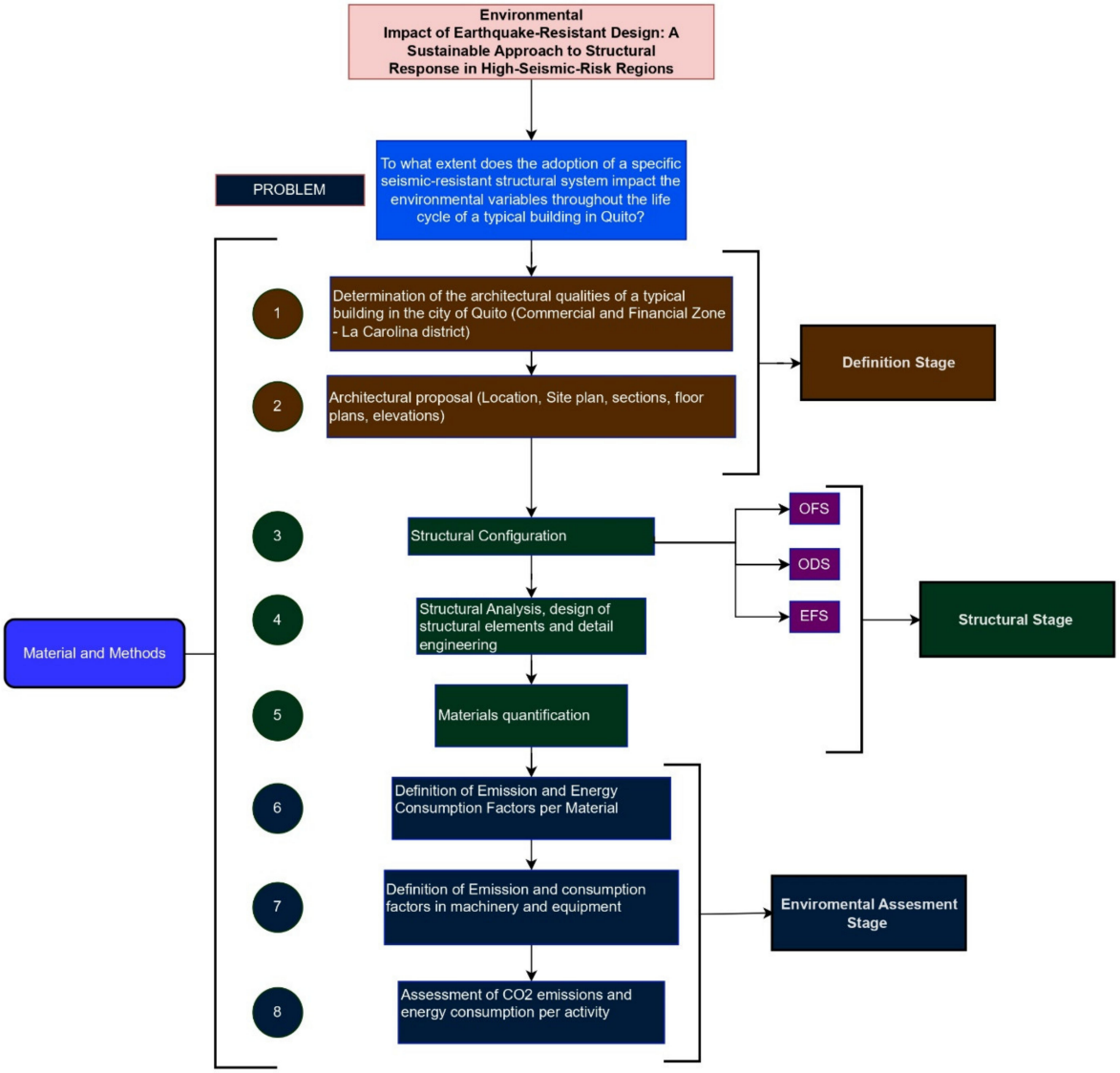


Figure 1. Flowchart illustrating the methodological framework for evaluating the environmental impact of seismic-resistant structural systems in a typical Quito building: from problem definition to environmental assessment.

Table 1. Dimensions and location of the case building study.

Parameter	Unit	Magnitude
Latitude	°	−0.178332
Longitude	°	−78.436299
Number of floors	u	7
Number of basements	u	3
Height without basements	m	18.55
Total height (including basements)	m	26.50
Floor area	m^2	255.43
Total floor area	m^2	4150.1
Bearing capacity	MPa	0.18

2.2. Structural Design Alternatives

The selection of structural systems in this study is grounded in the prevalent practices and regulations of the Ecuadorian construction sector, with a focus on story drift and structural resilience under seismic loading. The case study examines three structural

systems: the Optimized Frame System (OFS), the Optimized Dual System (ODS), and an alternative proposed system, the Equivalent Frame System (EFS) (Figure 2). The OFS and ODS are widely adopted in Ecuadorian construction and are comprehensively regulated by the Ecuadorian National Standards, which set minimum design requirements to ensure structural performance and occupant safety [35]. These standards mandate that building story drifts remain below 2% to minimize non-structural damage during seismic events. Evidence from the 2016 Pedernales earthquake in Ecuador demonstrated that, in frame systems, story drifts approaching 2% can lead to significant non-structural damage, increasing risks for building occupants.

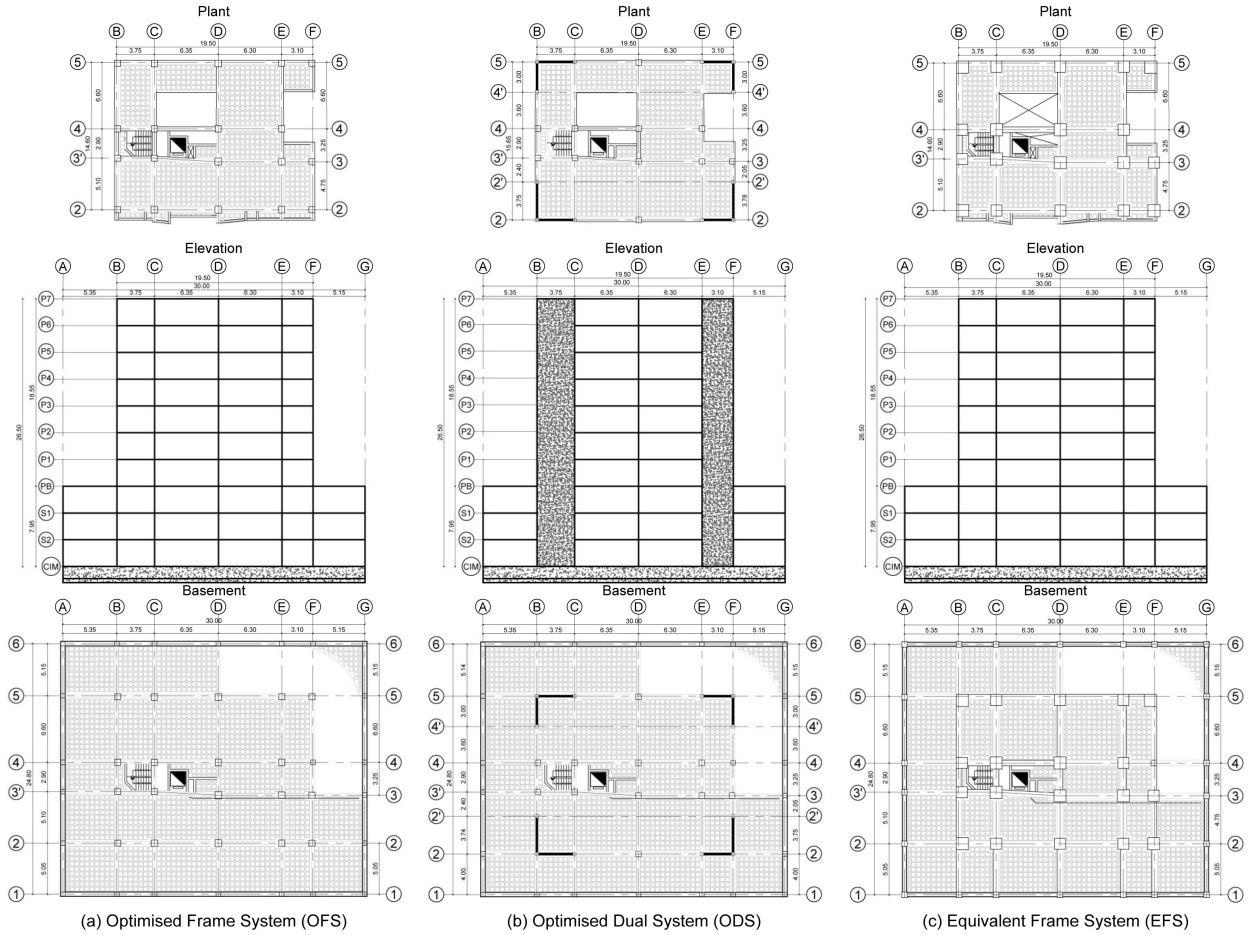


Figure 2. Structural configuration of the three systems: (**a**) the OFS, (**b**) ODS, and (**c**) EFS.

In contrast to the commonly used OFS and ODS, the EFS is a hypothetical, super-rigid frame system introduced in this study exclusively for comparative purposes. This system, which does not exist in current construction practices in Ecuador and has not been physically constructed, was conceptually designed to achieve a story drift comparable to the ODS. The EFS serves as a model to provide an additional level of rigidity, facilitating a controlled comparison of environmental impacts—such as carbon emissions and energy consumption—across systems with similar drift characteristics. By including the EFS in this analysis, this study offers a comprehensive evaluation of both structural performance and environmental impacts, aiding informed decision-making aimed at reducing carbon emissions while promoting structural performance in seismic-prone areas.

In this study, all three structural systems—the Optimized Frame System, the Equivalent Frame System, and the Optimized Dual System—were designed following Ecuadorian National Standards [36] to ensure compliance with local construction regulations. For the OFS and EFS, continuum sections with symmetric columns and beams were implemented

to maintain structural balance and uniformity. In the case of the ODS, proportionality in the length of the structural walls was carefully considered to optimize performance. The load calculations included a dead load of 4.42 kN/m^2 for the primary structural elements, while a superimposed dead load of 2.15 kN/m^2 accounted for permanent features like mezzanines and subfloors, with an additional 0.78 kN/m^2 for roofing materials. Based on the NEC-15 standards [37], a live load of 1.96 kN/m^2 was also incorporated to represent typical occupancy loads. Material properties were defined according to standard values: the yield stress of steel (fy) was set at 240 MPa, the compressive strength of concrete (f′c) at 28 MPa, and the allowable compressive strength of soil at 179.85 kN/m^2. The specified service loads (self-weight, permanent, and live loads in Table 2) and material properties (yield stress of steel at 420 MPa, concrete compressive strength at 28 MPa, and soil strength at 179.85 kN/m^2) ensure structural stability, compliance with seismic standards, and comparability across the OFS, ODS, and EFS systems, enabling the consistent assessment of drift performance under seismic loads.

Table 2. Detail of service loads and mechanical properties of materials.

Description	Magnitude	Units
Self-weight of slab	4.42	kN/m^2
Permanent mezzanine loads	2.15	kN/m^2
Permanent roof load	0.78	kN/m^2
Total dead load of mezzanine	6.57	kN/m^2
Total dead load of roof	5.20	kN/m^2
Live load	1.96	kN/m^2
Yield stress of reinforcing steel (fy)	420	MPa
Compressive strength of concrete (f′c)	28	MPa
Allowable compressive strength of soil	179.85	kN/m^2

Note: kN/m^2 indicates the load applied per unit area, measured in kilonewtons per square meter (kN/m^2).

The structural components—such as stairs, vehicular ramps, retaining walls, and roof slabs—were standardized across the three structural systems to ensure consistency in the comparative analysis. The staircase was designed with 15 cm thick roof slabs, treads of 25 cm, and risers of 19 cm. The vehicular ramp, constructed with a deck system, had a 12.5% slope and a thickness of 15 cm. Retaining wall thicknesses varied according to subsoil conditions, with dimensions of 35 cm, 40 cm, and 45 cm across different layers.

The roof slab system featured a two-way slab with a 5 cm compressive layer, supported by structural joists measuring 10 × 20 cm. This slab system incorporated voided slabs formed by 40 × 40 × 20 cm concrete blocks, ensuring structural efficiency while reducing material usage.

For seismic design, each structure's response to lateral forces was analyzed through both static and dynamic methods. Dynamic response analysis utilized the Square Root of the Sum of the Squares method to integrate torsional effects and higher vibration modes, accounting for complex dynamic behaviors. Seismic loads were calculated based on site-specific seismic hazards in accordance with Ecuadorian standards [37]. The dynamic effects were modeled using a design response spectrum, incorporating a portion of the structure's critical damping ratio [37].

The seismic-resistant design for all three systems aimed to prevent collapse during earthquakes, prioritizing occupant safety. To meet this objective, each system was engineered to resist seismic forces, maintain story drifts below the 2% limit prescribed by Ecuadorian standards [37], and effectively dissipate inelastic deformation energy (Table 3). This approach aligns with the design philosophy of resilience in seismic-prone regions, ensuring both structural stability and life safety.

Table 3. Structural variables per system.

System	Material	Period		Vibration Modes			Reactive Weight [kN]	Base Shear [kN]	Max Story Drift in X [%]
		ETABS [s]	NEC-15 [s]	1st in X	2nd in Y	3rd in RZ			
OFS	RC	0.834	0.762	73%	77%	73%	19,721	2716	1.75
ODS	RC	0.538	0.492	66%	67%	67%	18,652	3079	0.83
EFS	RC	0.541	0.762	69%	73%	71%	35,255	5344	0.82
OFS–EFS (% Difference)	-	35%	35%	10%	13%	8%	3%	-	53%
ODS–EFS (% Difference)	-	1%	35%	4%	8%	7%	42%	-	1%

Note: X is displacement across the X-axis; Y is displacement across the Y-axis; RZ is rotation around the Z axis; Reactive weight is the total weight of the superstructure; Max drift in X is the largest drift corresponding to the X-axis; RC is reinforced concrete.

2.3. Structural Design

Reinforce concrete elements sections and steel-reinforcement were quantified using [36,38] and the Load and Resistance Factor Design (LRFD) approach as it correlates the mechanical resistance of each component with the necessary resistance according to load combinations (Equation (1)). The equation shows that Rn is the nominal resistance, ϕ is the resistance factor, $\phi \cdot R_n$ is the resistance design, and $\sum(\lambda_i \cdot Q_i)$ is the most unfavorable stress.

$$\sum(\lambda_i \cdot Q_i) \leq \phi \cdot R_n \quad (1)$$

It is worth clarifying that the three structural systems share a similar design in the foundation beams due to the presence of multiple basement levels, as these contribute to reducing seismic moments on the foundation due to the lateral confinement provided by the soil. Differences in cross-sectional dimensions address specific stiffness and seismic resistance needs. In the EFS system, larger cross sections enhance stiffness and stability, helping withstand seismic forces with minimal deformation, similar to the ODS. Symmetry in cross sections is also key for uniform seismic force distribution, preventing stress concentrations that could affect safety, especially in T-shaped foundation beams and shear walls (Table 4).

2.4. Life Cycle Assessment of the Structural Systems

The life cycle assessment entails the evaluation of all the carbon emissions during the different phases to construct a building. In this study, we conduct a life cycle assessment of the three structural systems described above, which are the OFS, ODS, and EFS, to identify the system with the lowest carbon emission and energy consumption.

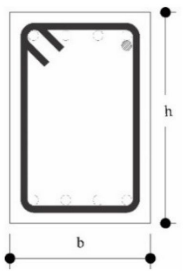
The most important environmental variable to evaluate the impact of human activities in nature is the emission of greenhouse gasses (i.e., CO_2 emissions) into the atmosphere. CO_2 emissions in the construction industry are not only limited to the construction phase of the building, but also to the manufacturing, production, transportation, and distribution processes of the construction materials. These stages were followed to agree with the PAS 2050:2011 [39] standard. A detailed view of the processes behind constructing a building is described in the process workflow (Figure 3).

2.4.1. Materials Quantification

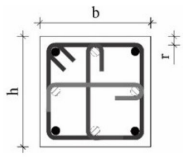
Each of the three structural systems—comprising beams, columns, stairs, walls, and slabs—contributes directly to the building's total carbon emissions across design, material sourcing, and construction phases. In this study, these components were constructed using materials like concrete, rebar steel, and wood (Table 5). In addition to the concrete elements, other sources of carbon emissions include excavation, soil disposal, and activities related to backfill material in foundations. Earthmoving activities—such as excavation, soil removal, and compaction—are measured in cubic meters and are essential preliminary steps in civil construction. Variations in foundation systems for each structural configuration affect the soil volumes required. Table 6 shows the soil volumes needed for each structural system's preconstruction activities, illustrating how these values depend on the foundation specifications.

Table 4. Final cross sections of structural systems. (a) beams and columns, (b) foundation beams and (c) structural walls.

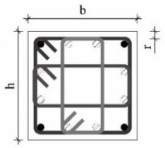
(a)



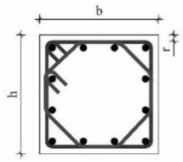
OFS			
Type of beam	b [cm]	h [cm]	r [cm]
V1 (P1-P7)	40	60	4
V2 (S2-PB)	30	50	4
V3 (S2-P7)	25	25	4
ODS			
V1 (P5-P7)	30	50	4
V2 (S2-P4)	35	55	4
V3 (S2-P7)	25	25	4
EFS			
V1 (S2-P7)	55	85	4
V2 (S2-P7)	25	40	4



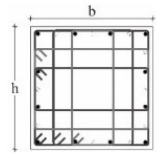
OFS			
Type of column	b [cm]	h [cm]	r [cm]
C1 (P5-P7)	50	50	4
C2 (P5-P7)	55	55	4
C3 (P5-P7)	50	55	4
C4 (P5-P7)	55	60	4
ODS			
C1 (P5-P7)	50	50	4



OFS			
C1 (PB-P5)	60	60	4
C2 (PB-P5)	65	65	4
C3 (PB-P5)	60	65	4
C4 (PB-P5)	65	70	4
ODS			
C1 (PB-P5)	55	55	4



OFS			
C1 (S3-PB)	60	60	4
C2 (S3-PB)	65	65	4
C3 (S3-PB)	60	65	4
C4 (S3-PB)	65	70	4
C5 (S3-PB)	45	45	3
ODS			
C1 (SB3-PB)	55	55	4



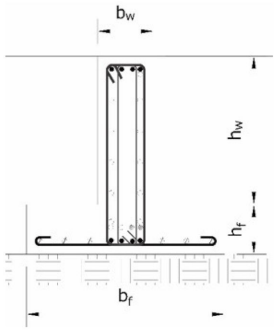
EFS			
Type of column	b [cm]	h [cm]	r [cm]
C1 (P5-P7)	110	110	4
C2 (P5-P7)	100	100	4
C1 (S3-P5)	120	120	4
C2 (P5-P7)	100	100	4

(b)

OFS				
Type of foundation beam	bf [cm]	hf [cm]	bw [cm]	hw [cm]
Inverted T Edge Beam	300	40	45	120
Inside Inverted T Beam	160	40	45	120
ODS				
Type of foundation beam	bf [cm]	hf [cm]	bw [cm]	hw [cm]
Inverted T Edge Beam	300	40	45	140
Inside Inverted T Beam	160	40	45	140
EFS				
Type of foundation beam	bf [cm]	hf [cm]	bw [cm]	hw [cm]
Inverted T Edge Beam	300	40	45	140
Inside Inverted T Beam	170	40	45	140

Table 4. *Cont.*

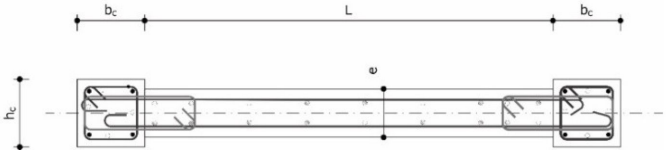
(b)



(c)

ODS

Type of wall	bc [cm]	hc [cm]	L [cm]	e [cm]
M1- Lower	35	35	340	25
M1- Upper	30	30	345	20
M2- Lower	35	35	265	25
M2- Upper	30	30	270	20
M3- Lower	35	35	275	25
M3- Upper	30	30	280	20



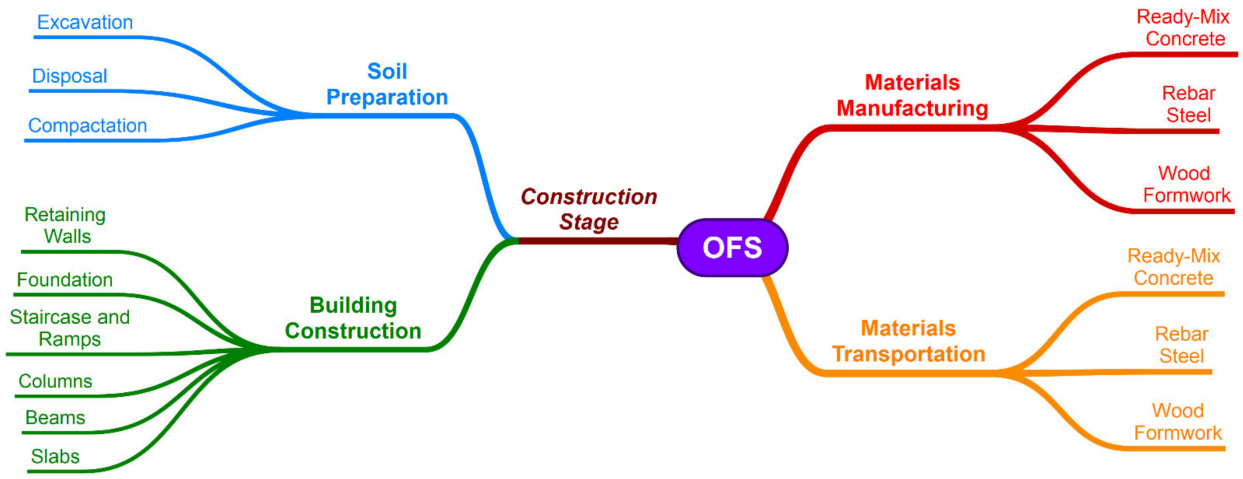


Figure 3. Work breakdown structure of the optimized frame system. The colors along each branch represent the different stages considered in the life cycle assessment process.

Table 5. Material quantities for key structural elements.

Structural Element	OFS			ODS			EFS		
	Concrete [m^3]	Rebar Steel [kg]	Wood Formwork [kg]	Concrete [m^3]	Rebar Steel [kg]	Wood Formwork [kg]	Concrete [m^3]	Rebar Steel [kg]	Wood Formwork [kg]
Retaining Walls	317.11	9720	2380	317.11	9770	2380	317.11	9720	2380
Foundation Beam	441.36	31,110	1540	473.47	50,920	1680	482.09	47,780	1660
Staircase and Ramps	62.86	12,070	570	62.86	12,070	570	62.86	12,070	0570
Beams	319.97	40,570	2670	257.24	19,420	2330	639.17	73,670	3680
Columns	214.22	47,740	2280	120.61	31,680	1430	704.54	155,280	4080
Shear Wall	-	-	-	205.24	27,480	2560	-	-	-
Slab	387.82	33,440	5380	392.29	33,530	5440	342.45	33,240	4750
Total	**1743.34**	**174,650**	**14,830**	**1828.83**	**184,860**	**16,390**	**2548.21**	**331,770**	**17,130**

Table 6. Quantification of soil involved during the construction phase. Soil activity.

Soil Activity	OFS	ODS	EFS
Excavation Volume [m^3]	7228.97	7228.97	7228.97
Unwanted material [m^3]	6017.83	6017.83	6017.83
Filling material [m^3]	769.78	737.67	729.05

2.4.2. Emission and Energy Consumption Factors per Material

The CO_2 emission factors (in kg of CO_2 per material unit) and energy consumption factors (in MJ per material unit) quantify the pollutants released during the fabrication of building materials, such as ready-mixed concrete or wooden formwork, and their impact on the environment. The assessment of these factors considered all stages involved in the fabrication of a building material, including the extraction of raw materials from the quarry and their transportation [20]. Table 7 provides the emission factor and energy consumption factor for the materials analyzed in this study. Concrete values are based on a compressive strength of 28 MPa, while rebar steel is specified with a yield strength of 420 MPa. MDP boards were chosen for formwork due to their versatility and reusability, allowing up to 10 uses per panel. The EF and ECF values were sourced from databases that best reflect the specific conditions of this case study [40–42].

Table 7. Emission and energy consumption factors in materials.

Material	EF [kg CO2 eq./u]	Source	Commentary	ECF [MJ/u]	Source
Concrete [m^3]	252	[41]	University of Bath Carbon and Energy Inventory f′c = 28 MPa	3623.190	[41]
Rebar Steel [kg]	1990	[41]	University of Bath Carbon and Energy Inventory	19,000.000	[42]
Wood Formwork [kg]	613	[20]	Study carried out at the University of La Coruña in MDP boards	3297.160	[20]

2.4.3. Emission and Consumption Factors in Machinery and Equipment

The construction industry relies heavily on machinery and instruments for various processes involved in building construction, such as materials transportation, soil compaction, and excavation. Most of the machinery used in construction runs on fossil fuels and electricity, which makes them significant sources of CO_2 emissions. The fuel efficiency of machinery was measured in liters of fuel per hour [20,43]. Equipment efficiency varies by project activity, measured in hours for on-site tasks and in kilometers for material transport (Table 8). Fuel efficiency directly affects the emissions produced by each piece of equipment. Additionally, multiple types of machinery, such as dump trucks and front loaders, may be needed for the same task, including excavation.

Table 8. Fuel efficiency in machinery and equipment.

Equipment and Machinery	Capacity	Efficiency [L/u]	Source
Dump Truck 6 × 4; 206 kW [km]	10 [m^3]	0.765	[43]
Cargo Truck [km]	50,000 [kg]	0.60	[43]
Concrete Mixer Truck; 3 axis; 221 kW [km]	8 [m^3]	0.77	[43]
Concrete Mixer Truck; 3 axis; 221 kW [h]	0.03 [h/m^3]	5.21	[20]
Vibratory plate compactor 5 kW [h]	0.53 [h/m^3]	1.10	[20]
Concrete vibrator (1.5″); 3 kW [h]	0.40 [h/m^3]	1.03	[20]
Backhoe 0.2 m^3; 45.6 kW [h]	0.05 [h/m^3]	5.21	[20]
Front Loader 1.5–1.7 and D3; 59 kW [h]	0.03 [h/m^3]	13.93	[20]
Concrete Pump 55.16 kW [h]	0.03 [h/m^3]	15.00	[20]

Sources of CO_2 emissions were classified based on their use in building construction, such as the transportation of equipment (e.g., trucks), construction machinery (e.g., concrete

mixer machine), and electric instruments (e.g., electric circular saw) [21,44]. Unlike internal combustion machinery, electrical equipment contributes less to environmental pollution. In Ecuador, this is especially relevant as much of the national grid's electricity comes from renewable hydroelectric power. Electric saws, in particular, are used for the precise cutting of materials like wood formwork and steel reinforcements (Tables 8 and 9).

Table 9. Electrical equipment power.

Equipment	Potency	Source
Chainsaw [W]	1200.00	[44]

CO_2 emissions from electric equipment are significantly lower than those from fossil fuels, making up approximately one-eighth of fossil fuel emissions [21]. The gas emission factor for diesel machinery (EF_{mch}) was determined by multiplying machinery fuel efficiency (n_{mch}) (Tables 8 and 9) by the diesel emission factor (EF_{diesel}) (Table 10), as shown in Equation (2). Similarly, the machinery energy consumption factor (ECF_{mch}) was calculated by multiplying the machinery fuel efficiency (Tables 8 and 9) with the diesel consumption factor (ECF_{diesel}, Table 10), as outlined in Equation (3).

Table 10. Emission and energy consumption factors due to the consumption of fuel (diesel) and electrical energy.

Energy Source	EF [kg of CO_2 eq./u]	ECF [MJ/u]	Source
Fuel (Diesel) [L]	2.5	34.68	[45]
Electric Power [MWh]	451	3600	[46]

Table 11 shows the emission and energy consumption factors for fuel use, such as diesel for internal combustion engines and electricity for electric motor equipment. Emission levels vary greatly between these sources, but it is important to note the different units—diesel emissions are measured per liter, while electricity emissions are measured per megawatt-hour (MWh), making direct comparisons challenging. In Ecuador, where much of the national electricity grid is powered by renewable hydroelectric sources, the environmental impact of electricity use is significantly lower than that of diesel.

$$EF_{mch} = n_{mch}\left[\frac{\text{L}}{\text{km}}\right] * EF_{diesel}\left[\frac{\text{kg of } CO_{2eq}}{\text{L}}\right] \quad (2)$$

$$ECF_{mch} = n_{mch}\left[\frac{\text{L}}{\text{km}}\right] * ECF_{diesel}\left[\frac{\text{MJ}}{\text{L}}\right] \quad (3)$$

Table 11. Emission and energy consumption factors in equipment and machinery.

Equipment and Machinery	EF [kg of CO_2 eq/u]	ECF [MJ/u]
Dump Truck 6 × 4, 10 m^3; 206 kW [km]	1.9	26.54
Cargo Truck 50,000 kg [km]	1.5	20.70
Concrete Mixer Truck; 3 axis; 8 m^3; 221 kW [km]	1.9	26.54
Concrete Mixer Truck; 3 axis; 221 kW [h]	13.1	180.68
Vibratory plate compactor 5 kW [h]	2.8	38.15
Concrete vibrator (1.5″); 3 kW [h]	2.6	35.72
Backhoe 0.2 m^3; 45.6 kW [h]	13.1	180.68
Front Loader 1.5–1.7 and D3; 59 kW [h]	35.1	483.09
Concrete Pump BSA 1000 1005 D3B C 55.16 kW [h]	37.8	520.20
Dump Truck 6 × 4, 10 m^3; 206 kW, [km]	0.5	4.32

2.4.4. Materials Transportation

Material transportation involves the movement of construction materials from the distribution depot to the building site [20]. Table 12 details the transportation requirements

for materials in this study, determined by material type and the specific truck type required. Total distance traveled—and consequently the environmental impact—is influenced by the load capacity and travel distance. Supplier proximity varies by construction site; for this study, transportation distances have been calculated based on the actual distance from the project location to the nearest supplier. The transportation analysis was conducted for ready-mixed concrete, steel reinforcement bars, and wooden formwork. Additionally, the transportation of waste from the building site to the construction material waste disposal site was also considered. The total distance traveled by the materials was computed by multiplying the number of trips (Equation (4) by the distance traveled.

$$Number\ of\ travels = \frac{Quantity\ of\ the\ required\ material\ (\text{units})}{Loading\ capacity\ of\ the\ transportation\ medium\ (\text{units})} \quad (4)$$

Table 12. Results of analysis of transport of materials in OFS.

Transportation	Type of Transport	u	Loading Capacity	Required Quantity	No. Trips [u]	Distance [km]	Total Distance [km]
Concrete	Concrete Mixer Truck; 3 axis; 8 m^3; 300 hp [km]	m^3	8	1743.34	436	7.8	3400.8
Rebar Steel	Cargo Truck 5000 kg [km]	kg	5000	174,650	70	6.2	434
Wood formwork	Cargo Truck 5000 kg [km]	kg	5000	14,830	6	2.3	13.8
Unwanted material	Dump Truck 6×4 m, 10 m^3; 280 hp [km]	m^3	10	6017.83	1204	12.5	15,050

2.4.5. Assessment of CO_2 Emissions and Energy Consumption per Activity

The evaluation of CO_2 emissions and energy consumption was conducted from the material fabrication stage through to the building's construction (Figure 2). To assess both the emission factor (EF) and energy consumption factor (ECF) for each activity, we propose an approach that considers the inputs from various pollution sources—such as machinery, materials, and transportation. This method allows for the conversion of units across these diverse sources into a unified activity work unit, as defined in Equations (5) and (6).

$$EF_{act} = (EF_{mch} + EF_m + EF_t)\left[\frac{\text{kg of } CO_{2eq}}{\text{u}}\right] \quad (5)$$

$$ECF_{act} = (ECF_{mch} + ECF_m + ECF_t)\left[\frac{\text{MJ}}{\text{u}}\right] \quad (6)$$

where

EF_{act}: emission factor per activity;
EF_{mch}: emission factor per machinery;
EF_m: emission factor per material;
EF_t: emission factor per transportation;
ECF_{act}: energy factor per activity;
ECF_{mch}: energy factor per machinery;
ECF_m: energy factor per material;
ECF_t: energy factor per transportation.

The calculation of the total emission per activity (TE_{act}) and total energy consumption factor (TEC_{act}) considers the product of the EF_{act} and ECF_{act} per activity by the total number of activities performed, respectively (Equations (7) and (8)). Table 13 shows the total emissions and energy consumption for each activity from material manufacturing to construction, using the OFS system as an example. It lists activity codes, descriptions, work units, quantities, and consolidated emission and energy factors that reflect the cumulative

environmental impact. Totals for CO_2 emissions and energy use are provided for each activity and the overall system, a method applied across all structural systems.

$$TE_{act} = EF_{act}\left[\frac{\text{kg of } CO_{2eq}}{\text{u}}\right] * quantity_{act}\ [\text{u}] \quad (7)$$

$$TEC_{act} = ECF_{act}\left[\frac{\text{MJ}}{\text{u}}\right] * quantity_{act}\ [\text{u}] \quad (8)$$

where

TE_{act}: total emission per activity;
TEC_{act}: total energy consumption per activity.

Table 13. Results of the environmental evaluation in the OFS.

No.	Code	Activity	u	Quantity	EF_{act}	ECF_{act}	Total Emission TE_{act}	Total Energy Consumption TEC_{act}
					[kg of CO_2 eq./u]	[MJ/u]	[$\times 10^3$ kg of CO_2 eq]	[MJ]
1	OFS-01-01	Materials Manufacturing						
2	OFS-01-01-01	Ready-mix concrete manufacturing	m^3	1743.34	252	3623.19	439.322	6,316,455.86
3	OFS-01-01-02	Rebar steel manufacturing	kg	174,650	1990	19,000	347.557	3,318,383.44
4	OFS-01-01-03	Wood formwork manufacturing	kg	14,830	613	3297.16	9.091	48,899.32
5	OFS-01-02	Transport of Materials						
6	OFS-01-02-01	Transport ready-mix concrete	km	3400.8	1.9	26.54	6.554	90,272.39
7	OFS-01-02-02	Transport rebar steel	km	434	1.5	20.7	0.652	8985.83
8	OFS-01-02-03	Transport wood formwork	km	13.8	1.5	20.7	0.021	285.72
9	OFS-01-03	Construction						
10	OFS-01-03-01	Earth Moving						
11	OFS-01-03-01-01	Excavation	m^3	7228.97	0.7	9.03	4.741	65,307.51
12	OFS-01-03-01-02	Eviction of unwanted material	m^3	6017.83	4.8	66.39	29.003	399,494.08
13	OFS-01-03-01-03	Soil compaction	m^3	769.78	1.5	20.22	1.13	15,563.67
14	OFS-01-03-02	Structure						
15	OFS-01-03-02-01	Retaining Walls						
16	OFS-01-03-02-01-001	Pouring concrete in retaining walls f′c = 280 kg/cm^2, includes pump transport	m^3	317.11	2.6	36.27	0.835	11,500.82
17	OFS-01-03-02-01-002	Reinforcing steel cutting fy = 4200 kg/cm^2	kg	9720	1.1	8.64	0.011	84.02
18	OFS-01-03-02-01-003	Formwork wood cutting of retaining walls	kg	2380	2.2	17.28	0.005	41.1
19	OFS-01-03-02-02	Foundation						
20	OFS-01-03-02-02-001	Pouring concrete in foundation beams f′c = 280 kg/cm^2, includes pump transport	m^3	441.36	2.5	33.94	1.088	14,981.44
21	OFS-01-03-02-02-002	Reinforcing steel cutting fy = 4200 kg/cm^2	kg	31,110	1.6	12.96	0.05	403.14
22	OFS-01-03-02-02-003	Formwork wood cutting of foundation beams	kg	1540	2.7	21.6	0.004	33.36
23	OFS-01-03-02-03	Staircase and Ramps						
24	OFS-01-03-02-03-001	Pouring concrete in staircase and ramps f′c = 280 kg/cm^2, includes pump transport	m^3	62.86	6.1	84.59	0.386	5317.65
25	OFS-01-03-02-03-002	Reinforcing steel cutting fy = 4200 kg/cm^2	kg	12,070	1.1	8.64	0.013	104.28
26	OFS-01-03-02-03-003	Formwork wood cutting of staircase and ramps	kg	570	2.2	17.28	0.001	9.93
27	OFS-01-03-02-04	Columns						
28	OFS-01-03-02-04-001	Column pouring concrete f′c = 280 kg/cm^2, includes pump transport	m^3	214.22	3.5	48.29	0.751	10,344.58
29	OFS-01-03-02-04-002	Reinforcing steel cutting fy = 4200 kg/cm^2	kg	47,740	1.6	12.96	0.077	618.75
30	OFS-01-03-02-04-003	Formwork wood cutting of columns	kg	2280	2.7	21.6	0.006	49.23
31	OFS-01-03-02-05	Beams						
32	OFS-01-03-02-05-001	Pouring concrete in beams f′c = 280 kg/cm^2, includes pump transport	m^3	319.97	3.1	43.31	1.006	13,856.79
33	OFS-01-03-02-05-002	Reinforcing steel cutting fy = 4200 kg/cm^2	kg	40,570	1.6	12.96	0.066	525.82
34	OFS-01-03-02-05-003	Formwork wood cutting of beams	kg	2670	2.7	21.6	0.007	57.73
35	OFS-01-03-02-06	Slabs						
36	OFS-01-03-02-06-001	Pouring concrete in slabs f′c = 280 kg/cm^2, includes pump transport	m^3	387.82	3	41.54	1.17	16,110.24
37	OFS-01-03-02-06-002	Reinforcing steel cutting fy = 4200 kg/cm^2	kg	33,440	1.1	8.64	0.036	288.88
38	OFS-01-03-02-06-003	Formwork wood cutting of slabs	kg	5380	2.2	17.28	0.012	92.99
		Total:					**843.6**	**10,338,068.58**

3. Results

3.1. Overall Results

The evaluation of CO_2 emissions showed that the EFS system produced the highest emissions compared to the OFS and ODS systems. The emissions in the EFS system were approximately 39% higher (around 480,000 kg) than the emissions in the OFS and ODS systems (Figure 4). This increase is largely due to the structural demands of the EFS

system, which is a rigid frame design intended to match the performance levels of the OFS and ODS systems. To achieve this equivalent structural capacity, the EFS requires significantly more material and construction resources than the optimized systems. In terms of material-related emissions, the OFS system generated 439.32 $\times$ 10^3 kg of CO_2 from premixed concrete and 347.55 $\times$ 10^3 kg of CO_2 from rebar steel. Similarly, the ODS system resulted in 460.86 $\times$ 10^3 kg of CO_2 from concrete and 367.87 $\times$ 10^3 kg of CO_2 from rebar steel. In contrast, the EFS system produced 642.15 $\times$ 10^3 kg of CO_2 for concrete and 660.23 $\times$ 10^3 kg of CO_2 for rebar steel, reflecting the additional material usage required to meet the desired structural performance. Between the OFS and ODS systems, the emissions of CO_2 in the ODS system were approximately 5% higher (around 43,000 kg) than in the OFS system (Figure 3). Energy consumption (Figure 4) showed a similar trend in comparison with the EFS, OFS, and ODS systems, with the highest consumption in the EFS system at around 58% (around 6 million MJ) higher than in the OFS and ODS systems. Similarly to CO_2 emissions, the ODS system consumed slightly more energy (around 6%) than the OFS system.

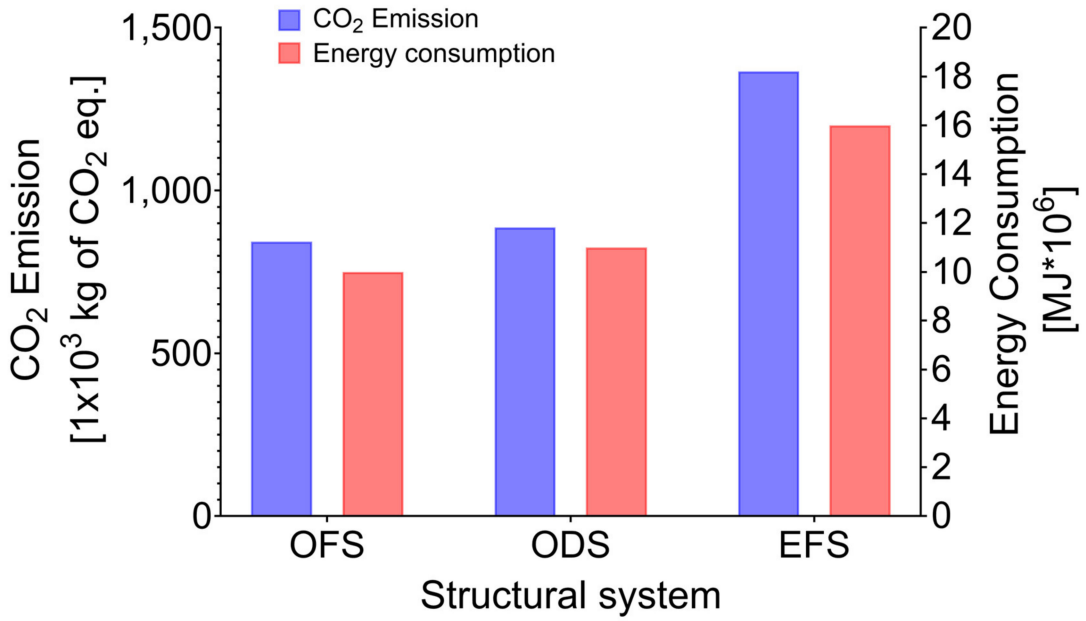


Figure 4. CO_2 emission and energy consumption per structural system.

3.2. A Detailed Description of Results per Building Stage

The life cycle assessment showed that the EFS system had the highest CO_2 emissions and energy consumption compared with the OFS and ODS systems (Section 3.1). The assessment considered the stages of material fabrication, transportation, and building construction, with the fabrication stage accounting for the largest CO_2 emissions and energy consumption (Figure 5). The differences in CO_2 emissions and energy consumption between the OFS and ODS systems were insignificant across stages, except for the fabrication stage where the ODS system had 5% higher emissions and consumption than the OFS system (Figure 5). When comparing the OFS and ODS systems with the EFS system, the fabrication stage accounted for over 40% of the total CO_2 emissions and energy consumption.

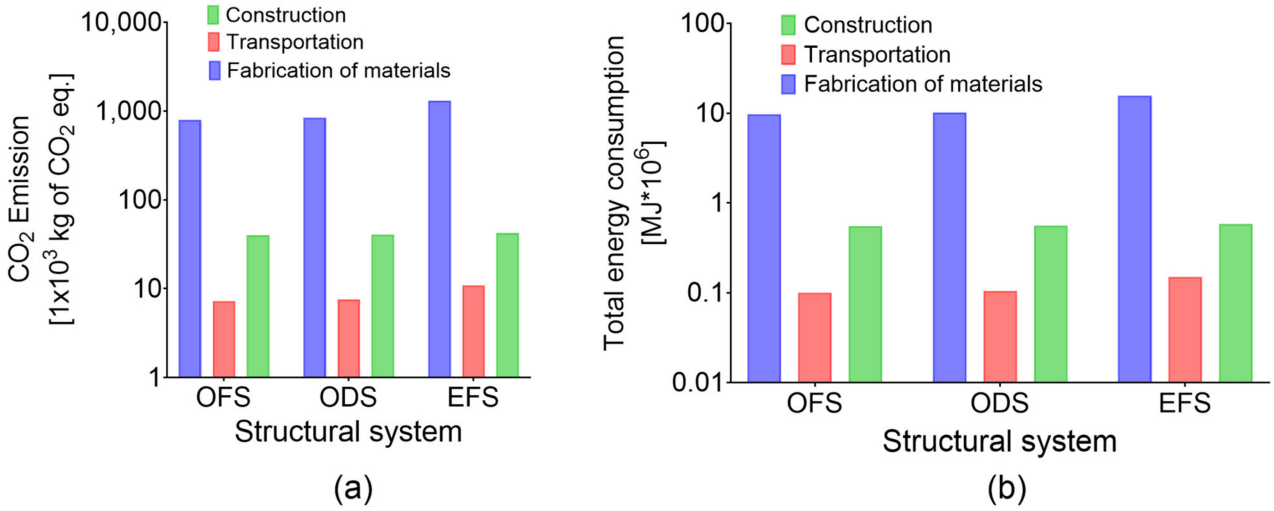


Figure 5. (**a**) CO_2 emission per activity in each structural system and (**b**) total energy consumption per activity in each structural system.

3.3. Influence of the Material on the Emission of CO_2 and Energy Consumption

The influence of materials on the emission of CO_2 and energy consumption considers the impact of ready-mixed concrete, steel rebar reinforcement, wooden formwork, and soil-related activities in the three structural systems (OFS, ODS, and EFS). Results showed that ready-mixed concrete and steel rebar reinforcement are the main contributors to CO_2 emissions and energy consumption, accounting for more than 50% and 40% of overall emissions, respectively (Figure 6). Wooden formwork and soil removal activities have a relatively small impact, contributing to less than 1% and 5% of emissions, respectively. Notably, in the EFS system, steel rebar reinforcement and ready-mixed concrete have similar CO_2 emissions, with steel rebar reinforcement emissions being slightly higher (around 0.5%) than ready-mixed concrete emissions (Figure 6). In contrast, in the OFS and ODS systems, ready-mixed concrete was the main source of CO_2 emissions, accounting for 27% more emissions than steel rebar reinforcement. Based on the overall contribution of materials to CO_2 emissions and energy consumption, the structural systems can be ranked from having the highest to lowest environmental impact as follows: EFS, ODS, and OFS.

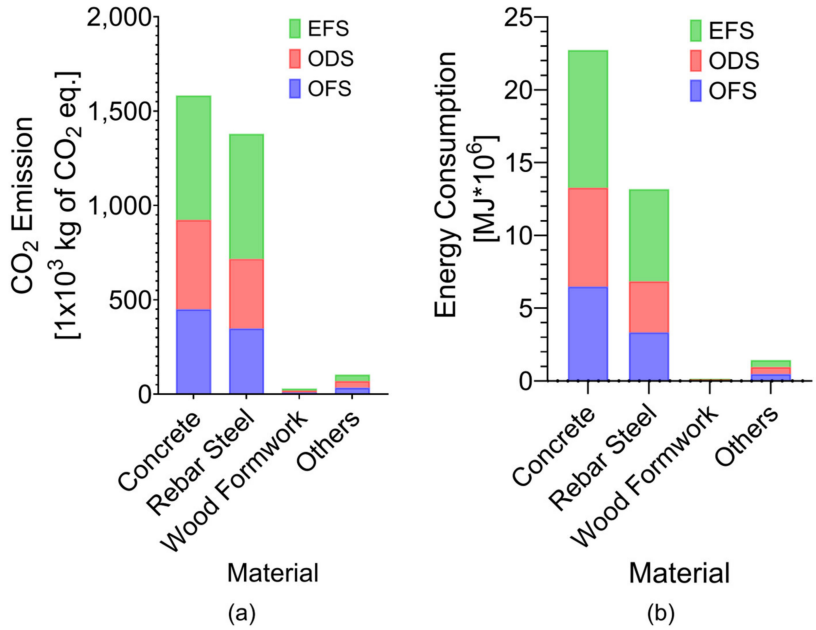


Figure 6. (**a**) CO_2 emission per material and (**b**) total energy consumption per material.

3.4. Environmental Impact of the Structural Elements Used in Each Structural System

The structural elements that contribute the most to CO_2 emissions and energy consumption in the OFS and ODS systems are the foundation, beams, and slabs (Figure 7). In the OFS system, foundation beams account for around 22% of the total CO_2 emissions and 22.7% of the total energy consumption. In the ODS system, these figures increase to approximately 26.4% and 26.3%, respectively. In the EFS system, foundation beams contribute to around 16% of the total CO_2 emissions and 17% of the total energy consumption (Figures 7 and 8). Notably, in the EFS system, columns and beams, rather than foundation beams, are the main sources of CO_2 emissions and energy consumption, which are roughly two times higher than those produced by foundation beams. This difference in results is due to the modifications made to the columns and beams in the EFS system to reduce drift and achieve a similar structural response to the ODS system, allowing for a better assessment of the impact of materials and energy on the EFS system's environmental impact.

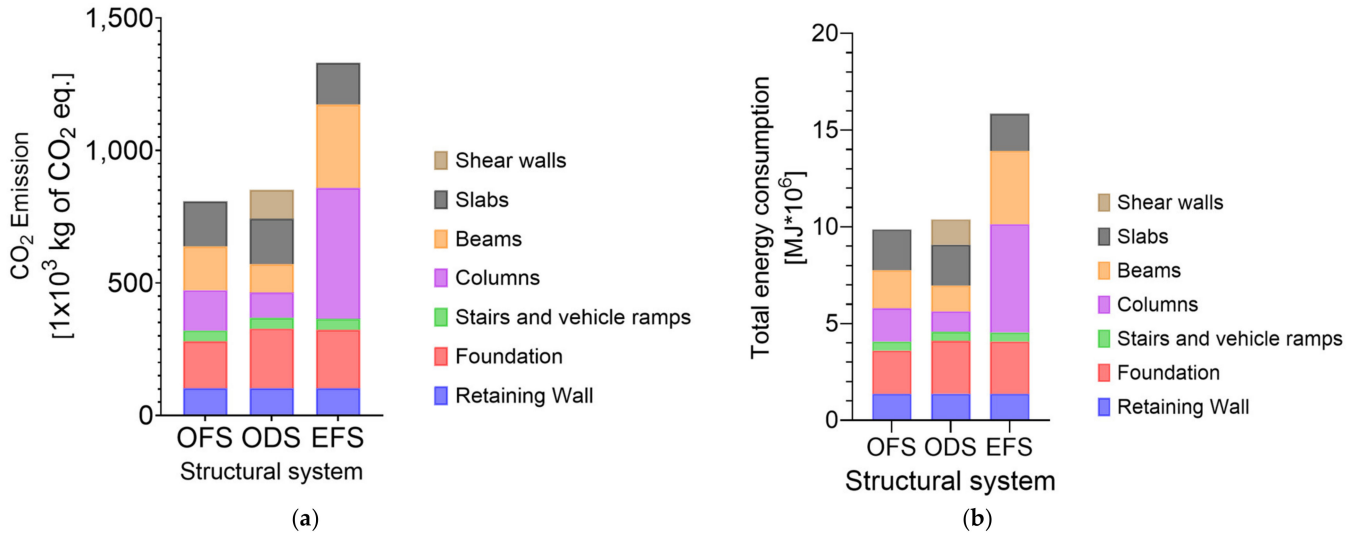


Figure 7. (**a**) CO_2 emission per structural element and (**b**) total energy consumption per structural element.

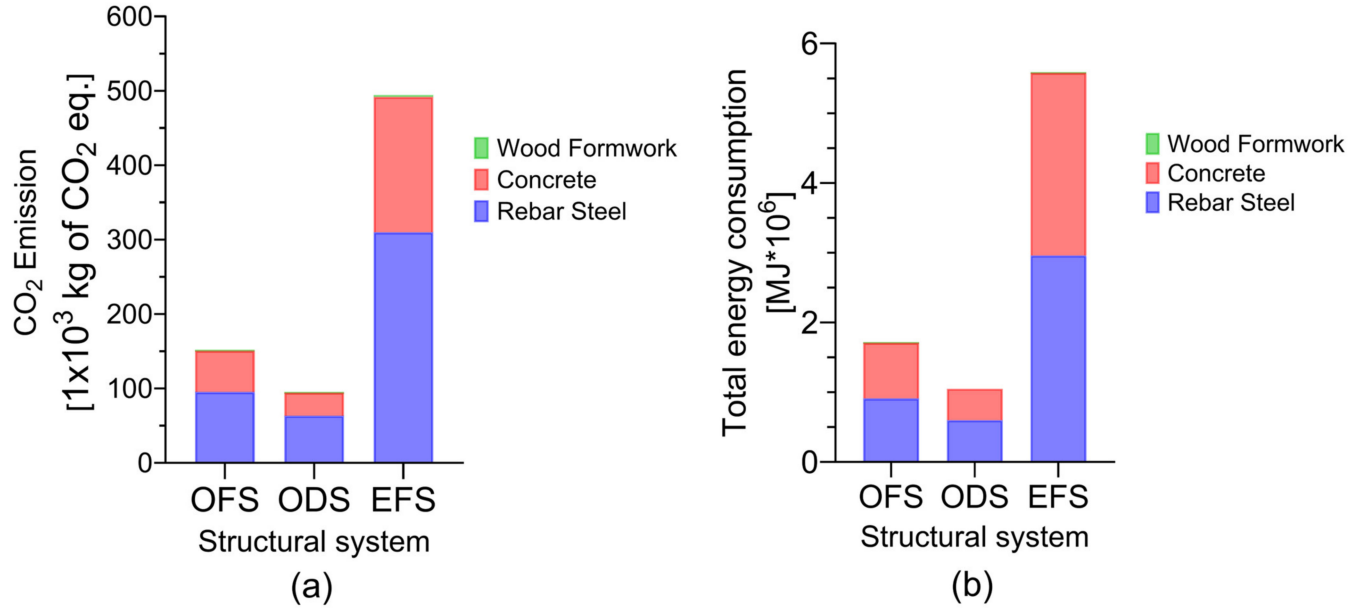


Figure 8. (**a**) CO_2 emission in structural system and material by columns and (**b**) total energy consumption in structural system and material by columns.

Further analysis of the components of the structural elements in terms of the materials used showed that steel reinforcement in columns (maximum reinforcement ratio elements) accounts for approximately 64% and 54% of CO_2 emissions and energy consumption, respectively, in all three structural systems. In contrast, ready-mixed concrete is the main source of emissions in minimum reinforcement ratio elements, such as slabs, contributing to around 58% and 68% of CO_2 emissions and energy consumption, respectively (Figures 7 and 8). Therefore, steel is the primary source of emissions in maximum reinforcement ratio elements, while ready-mixed concrete is the main source in minimum reinforcement ratio elements.

4. Discussion

The design and construction of buildings is a complex process that requires consideration of various technical factors, including mechanical resistance, environmental impact, and sustainability [20,21,47,48]. While traditional building design in developing countries has focused primarily on structural design, it has largely neglected environmental factors such as emissions of CO_2 and energy consumption [49,50]. This has led to buildings that are likely to be environmentally inefficient. The study discussed in this article is the first of its kind in Ecuador, comparing the carbon footprint of different structural systems (OFS and ODS) with an equivalent structure (EFS). The results of this study provide evidence of how structural decisions made into the design of building structures could incur higher or lower levels of pollution, focusing on the context of developing country with a high seismic risk.

There is a notable impact of the materials utilized on CO_2 emissions and energy consumption within the construction industry. The use of different materials such as concrete, steel, and wood can have different environmental impacts. For instance, concrete has a high carbon footprint due to the production of cement, which is one of the major contributors to CO_2 emissions. In contrast, wood has a lower carbon footprint due to its renewable nature and the ability to store carbon. In addition to the type of material, the origin of the material also plays a role in the emission of CO_2 and energy consumption. Materials that are sourced locally have a lower carbon footprint compared to materials that are transported from distant locations. This is because the transportation of materials consumes energy and emits CO_2, adding to the overall environmental impact of the building. Furthermore, the durability and maintenance requirements of the materials used can also impact the emission of CO_2 and energy consumption. Materials that require frequent maintenance and replacement can have a higher environmental impact compared to materials that are durable and require less maintenance. Research by Resch et al. (2020) [51] found that the transportation of materials significantly contributes to CO_2 emissions in building construction, averaging around 6%. Overall, the choice of materials used in construction can have a significant impact on the emission of CO_2 and energy consumption. Sustainable and eco-friendly materials, sourced locally and with low maintenance requirements, can reduce the environmental impact of the building.

The life cycle assessment (Figure 4) revealed that the Optimized Frame System demonstrated the lowest CO_2 emissions and energy consumption among the three structural systems evaluated. However, while its story drift of 1.75% complies with the Ecuadorian standard [52], which allows drifts below 2%, the earthquake-resistant performance remains concerning. Damage associated with rigid masonry at this level of drift has led to severe consequences, including fatalities, as seen in the 2016 Pedernales earthquake [35]. Optimal design in this context refers to achieving a balance between minimizing environmental impact (CO_2 emissions and energy consumption) and maximizing structural resilience (minimizing drift) to meet safety standards during seismic events. Based on these criteria, the Optimized Dual System stands out as the optimal solution, as it provides the best compromise between these competing demands.

The ODS system demonstrated a compelling balance between environmental impact and structural resilience, despite slightly higher CO_2 emissions (5%) and energy consump-

tion (6%) compared to the OFS. Specifically, the drift analysis reveals that the ODS system achieved a story drift of 0.82%, which is less than half the drift experienced in the OFS system (1.75%). This lower drift significantly enhances the earthquake-resistant performance by limiting the damage to non-structural components, which, as studies have shown [53,54], are often critical factors in building safety and occupant protection during seismic events. By reducing drift, the ODS system helps preserve the integrity of non-structural elements, minimizing risks associated with injury or fatality due to non-structural failures. Furthermore, while the EFS presents a similar drift to the ODS, its CO_2 emissions and energy requirements are substantially higher, increasing by approximately 54% and 51%, respectively, compared to the ODS. This environmental cost makes the EFS less favorable when considering a comprehensive approach to sustainability. Thus, the ODS system stands out as the most suitable solution, achieving both resilience in seismic conditions and a relatively low environmental footprint.

There is a direct relationship between the need to create more rigid structures to mitigate the effects of seismic forces and pollution levels. In this sense, the EFS is a clear example of an ill-advised way to generate a rigid structure, as it incurs in high levels of pollution. A similar finding was reported in a life cycle assessment of buildings in Atlanta, USA, where energy consumption and CO_2 emissions increased in more complex, heavier, and rigid structures compared to lighter structures [20]. Therefore, it is necessary to seek a balanced approach to forming a rigid structure with low pollution levels, as achieved with the ODS. Regardless of the chosen structural system (EFS, OFS, and ODS), the maximum CO_2 emissions and energy consumption (about 90%) were recorded during the materials fabrication stage. This can be attributed to industrial processes involved in material fabrication, such as steel melting and heat treatment, or cement clinker production. Previous studies examining the environmental impact of steel and concrete used in residential [48] and commercial buildings in Singapore [55] reported similar findings. It is worth noting that the location of the building has a significant impact on the materials fabrication stage. For instance, countries in the Circum-Pacific belt, known for their high seismic activity, require more robust structural systems, which requires more concrete, and steel, leading to higher CO_2 emissions and energy consumption during fabrication compared to areas with lower seismic activity such as the East Coast of the United States.

The production of concrete and steel, which are the primary materials used in each structural component that provides mechanical resistance, contributes significantly to carbon emissions and energy consumption. In the OFS and ODS systems, the major contributor to CO_2 emissions and energy consumption was the ready-mixed concrete. However, in the EFS system, despite the abundance of ready-mixed concrete, most of the emissions and consumption were caused by steel. This outcome can be attributed to the fabrication process of steel, which involves several heating processes, including melting and heat treatments, resulting in significant pollutant emissions [56]. In contrast, the fabrication of ready-mixed concrete requires only one heating process [57]. Moreover, the EFS system has large, robust structural elements that require substantial amounts of steel, altering the weight ratio between steel and ready-mixed concrete. The ratio is higher in the EFS than in the OFS and ODS systems, making steel reinforcement the primary contributor to CO_2 emissions.

Another notable difference between the optimized systems (OFS and ODS) and the EFS was the environmental impact of the structural elements. In the OFS and ODS systems, foundation beams and slabs accounted for the majority of emissions and energy consumption, while in the EFS, beams and columns were the main contributors of pollutants into the environment. This discrepancy could be explained by the balanced number of structural elements in the optimized systems, which resulted in no significant differences in emissions between them. However, in the EFS system, CO_2 emissions and the energy consumption of beams and columns were at least ten times higher than those of other structural elements (e.g., slabs). This highlights the fact that the EFS system requires more columns and beam elements (approximately 419% more columns and 190% more beams) to achieve a similar

story drift compared to the ODS system, which has a similar structural response with fewer columns and beams.

This study examined the structural behavior of three different systems and their impact on the environment. In developing countries, there is limited information available on how the structural system of buildings affects the environment, with most studies focusing on architectural design or the type of material used [23,24,29]. By incorporating environmental considerations into the design of structures, we offer a new methodology for creating sustainable buildings that significantly reduce the carbon footprint compared to traditional design approaches. Furthermore, we also assessed the structural behavior of these systems, with a focus on story drift as the primary structural variable. The ODS system, which combines the benefits of lower CO_2 emissions and lower story drift, underscores the significance of story drift in the structural response of the system and its environmental impact. This system offers the advantage of combining the low CO_2 emissions and energy consumption of the OFS system with the mechanical strength of the EFS system.

As the field of environmental impact assessment for buildings in Ecuador is still in its infancy and our study is the first to integrate earthquake-resistant design and environmental impact analysis, there is limited information available on the factors that contribute to CO_2 emissions and energy consumption during the construction process. To overcome this limitation, we relied on published databases to quantify the environmental impact of structural elements and materials in each of the three structural systems [40–42]. Furthermore, a more comprehensive life cycle assessment that takes into account the role of building occupants will provide additional insights into the environmental impact of new constructions.

Table 14 compares the results obtained in the different stages of the life cycle, as can be seen in each of the different studies in scope, some cover more stages, others less. However, in most studies [17,20,55] the results (maximum and minimum) are within the same order of magnitude, except for the study by Suzuki et al. (1995) [48] conducted in Japan.

Table 14. Comparison of the results obtained in the different stages of the life cycle.

Author	Location	Embodied Carbon of Concrete Structures [kg of CO_2 eq.]		
		Manufacture Phase	Transportation Phase	Construction Phase
Moussavi and Akbarnezhad, 2015 [20]	USA	548,000–847,000	37,000–58,000	50,000–66,000
Suzuki et al., 1995 [48]	Japan	2,232,000–3,034,000	-	-
Cole, 1998 [17]	Canada	-	33,000	29,000
Kua and Wong, 2012 [55]	Singapore	871,000	-	-
This study	Ecuador	796,000–1,313,000	7000–11,000	40,000–43,000

5. Conclusions

This study comprehensively evaluated the environmental impact and structural performance of three structural systems—EFS, OFS, and ODS—in terms of CO_2 emissions, energy consumption, and seismic resilience. The findings demonstrated significant differences in the environmental burdens associated with each system, primarily due to variations in material usage and structural configurations. Among the systems, the EFS generated the highest environmental impact, emitting approximately 39% more CO_2 and consuming 58% more energy than the OFS and ODS systems. This result was attributed to the substantial material demands of the EFS, specifically in steel and concrete, required to achieve similar structural stability.

The ODS system emerged as the optimal structural solution, offering a balanced approach with lower CO_2 emissions and energy consumption while delivering superior seismic resilience—achieving a 53% reduction in story drift compared to the OFS system. This result highlights the critical role of structural optimization in minimizing non-structural damage, which is essential for building safety and occupant protection during seismic events. The EFS system, by contrast, was designed hypothetically to illustrate the extent to

which structural elements must be scaled up to match the ODS's performance. Although the EFS achieved similar drift performance, it incurred significantly higher environmental costs, primarily due to the increased steel reinforcement required. This elevated environmental impact makes the EFS a less sustainable option, despite its comparable structural resilience to the ODS.

Our results emphasize that environmental impacts are predominantly generated during the materials fabrication stage, accounting for approximately 90% of total emissions and energy consumption. This highlights the urgent need for sustainable production practices, especially in high seismic risk regions like Ecuador, where structural demands are inherently higher.

This research introduces a new framework for sustainable structural design in developing countries, integrating both environmental considerations and seismic performance. Given the infancy of life cycle assessments in Ecuador, this study contributes essential insights into optimizing structural systems to minimize environmental impact without compromising resilience. The ODS system, offering a lower carbon footprint with enhanced seismic performance, is recommended for future building designs in Quito, demonstrating a practical pathway to achieving sustainable, earthquake-resistant structures. The findings call for updated design guidelines that prioritize efficient material use, promote low-emission production techniques, and foster resilient infrastructure to meet the evolving challenges of environmental sustainability and seismic safety in urban development.

Supplementary Materials: The following supporting information can be downloaded at: https://www.mdpi.com/article/10.3390/buildings14123821/s1.

Author Contributions: A.B.: conceptualization, writing draft, data collection, analysis of results, definition of methodology. E.V.: conceptualization, writing draft, data collection, analysis of results, definition of methodology. E.R.: conceptualization, writing—review and editing, supervision. C.A.: conceptualization, Writing—review and editing, supervision, analysis of results, definition of methodology. All authors have read and agreed to the published version of the manuscript.

Funding: This research received no external funding.

Data Availability Statement: The data that support the findings of this study are available from the corresponding author C.A. upon reasonable request.

Conflicts of Interest: The authors declare no conflicts of interest.

References

1. Işık, E.; Avcil, F.; İzol, R.; Büyüksaraç, A.; Bilgin, H.; Harirchian, E.; Arkan, E. Field Reconnaissance and Earthquake Vulnerability of the RC Buildings in Adıyaman during 2023 Türkiye Earthquakes. *Appl. Sci.* **2024**, *14*, 2860. [CrossRef]
2. Ivanov, M.L.; Chow, W.-K. Structural damage observed in reinforced concrete buildings in Adiyaman during the 2023 Turkiye Kahramanmaras Earthquakes. *Structures* **2023**, *58*, 105578. [CrossRef]
3. Smith, E.M.; Mooney, W.D. A seismic intensity survey of the 16 April 2016 Mw7.8 Pedernales, Ecuador, Earthquake: A comparison with strong-motion data and teleseismic backprojection. *Seismol. Res. Lett.* **2021**, *92*, 2156–2171. [CrossRef]
4. Viteri, C.V.; Bravo, Y.M.; Gutiérrez, D.D.; Moreira, S.A. A Look at the Traditional Construction During the Earthquake of 7.8 Mw of Pedernales 2016 (Ecuador): The Case of Portoviejo City. In *Sustainability and Automation in Smart Constructions: Proceedings of the International Conference on Automation Innovation in Construction (CIAC-2019), Leiria, Portugal, 7–8 November*; Springer International Publishing: Berlin/Heidelberg, Germany, 2021; pp. 363–375. [CrossRef]
5. Gonzalez, R.E.; Stephens, M.T.; Toma, C.; Dowdell, D. The Estimated Carbon Cost of Concrete Building Demolitions following the Canterbury Earthquake Sequence. *Earthq. Spectra* **2022**, *38*, 1615–1635. [CrossRef]
6. Shafieezadeh, A.; Ivey Burden, L. Scenario-based resilience assessment framework for critical infrastructure systems: Case study for seismic resilience of seaports. *Reliab. Eng. Syst. Saf.* **2014**, *132*, 207–219. [CrossRef]
7. Welsh-Huggins, S.J.; Liel, A.B. A life-cycle framework for integrating green building and hazard-resistant design: Examining the seismic impacts of buildings with green roofs. *Struct. Infrastruct. Eng.* **2017**, *13*, 19–33. [CrossRef]
8. Gonzalez, R.E.; Stephens, M.T.; Toma, C.; Dowdell, D. Incorporating potential environmental impacts in building seismic design decisions. *Bull. Earthq. Eng.* **2023**, *21*, 4385–4428. [CrossRef]
9. Silva, V.; Akkar, S.; Baker, J.; Bazzurro, P.; Castro, J.M.; Crowley, H.; Dolsek, M.; Galasso, C.; Lagomarsino, S.; Monteiro, R.; et al. Current Challenges and Future Trends in Analytical Fragility and Vulnerability Modeling. *Earthq. Spectra* **2019**, *35*, 1927–1952. [CrossRef]

10. Ruggieri, S.; Calò, M.; Cardellicchio, A.; Uva, G. Analytical-mechanical based framework for seismic overall fragility analysis of existing RC buildings in town compartments. *Bull. Earthq. Eng.* **2022**, *20*, 8179–8216. [CrossRef]
11. Del Gaudio, C.; Di Ludovico, M.; Polese, M.; Manfredi, G.; Prota, A.; Ricci, P.; Verderame, G.M. Seismic fragility for Italian RC buildings based on damage data of the last 50 years. *Bull. Earthq. Eng.* **2020**, *18*, 2023–2059. [CrossRef]
12. Kim, S.; Moon, J.H.; Shin, Y.; Kim, G.H.; Seo, D.S. Life comparative analysis of energy consumption and CO_2 emissions of different building structural frame types. *Sci. World J.* **2013**, *2013*, 175702. [CrossRef] [PubMed]
13. Architecture 2030. Why The Building Sector? Available online: https://architecture2030.org/why-the-building-sector/ (accessed on 22 September 2022).
14. Ritchie, H.; Rosado, P.; Roser, M. CO_2 and Greenhouse Gas Emissions. 2020. Available online: https://ourworldindata.org/co2-and-greenhouse-gas-emissions (accessed on 22 September 2022).
15. Google; Ellen MacArthur Foundation. *Accelerating the Circular Economy Through Commercial Deconstruction and Reuse*, 1st ed.; Ellen MacArthur Foundation: Cowes, UK, 2019; pp. 1–23.
16. Anink, D.; Boonstra, C.; Mak, J.; Morris, A. *Handbook of Sustainable Building: An Environmental Preference Method for Selection of Materials for Use in Construction and Refurbishment*; Undefined; James & James: Springdale, AR, USA, 1996.
17. Cole, R.J. Energy and greenhouse gas emissions associated with the construction of alternative structural systems. *Build. Environ.* **1998**, *34*, 335–348. [CrossRef]
18. Galatowitsch, S.M. Carbon Offsets as Ecological Restorations. *Restor. Ecol.* **2009**, *17*, 563–570. [CrossRef]
19. Harmouche, N.; Ammouri, A.; Srour, I.; Chehab, G.; Hamade, R. Developing a carbon footprint calculator for construction buildings. In *Construction Research Congress 2012: Construction Challenges in a Flat World, Proceedings of the 2012 Construction Research Congress, West Lafayette, IN, USA, 21–23 May 2012*; ASCE: Reston, VA, USA, 2012; pp. 1689–1699. [CrossRef]
20. Moussavi Nadoushani, Z.S.; Akbarnezhad, A. Effects of structural system on the life cycle carbon footprint of buildings. *Energy Build.* **2015**, *102*, 337–346. [CrossRef]
21. Paik, I.; Na, S. Comparison of Carbon Dioxide Emissions of the Ordinary Reinforced Concrete Slab and the Voided Slab System During the Construction Phase: A Case Study of a Residential Building in South Korea. *Sustainability* **2019**, *11*, 3587. [CrossRef]
22. Auburtin, P.N.; Saadé, M.; Manthey, M.; Louërat, M.; Martin, J.-L.; Baverel, O. Influence of building geometry on the environmental impact of building structures. *J. Phys. Conf. Ser.* **2023**, *2600*, 152001. [CrossRef]
23. Güereca, L.P. *Evaluación de la Huella de Carbono con Enfoque de Análisis de Ciclo de Vida para 12 Sistemas Constructivos*; REPORTE FINAL (Versión 2.0 que Incluye Correcciones de Block Cerámico); Instituto de Ingenieria (UNAM): Mexico City, Mexico, 2016.
24. Casaverde, R. Cuantificación De CO_2 Generado Por El Consumo Energético En La Construcción De Viviendas Unifamiliares—SATIPO. Ph.D. Thesis, Universidad Nacional Del Centro Del Perú, Huancayo, Peru, 2016.
25. Luo, C.; Yao, X.; Zhang, Y.; Zhou, H. An Empirical Study on the Impact of Different Structural Systems on Carbon Emissions of Prefabricated Buildings Based on SimaPro. *World J. Eng. Technol.* **2023**, *11*, 434–453. [CrossRef]
26. Dash, M.K.; Patro, S.K. Effects of water cooled ferrochrome slag as fine aggregate on the properties of concrete. *Constr. Build. Mater.* **2018**, *177*, 457–466. [CrossRef]
27. Karalar, M.; Bilir, T.; Çavuşlu, M.; Özkiliç, Y.O.; Sabri Sabri, M.M. Use of recycled coal bottom ash in reinforced concrete beams as replacement for aggregate. *Front. Mater.* **2022**, *9*, 1064604. [CrossRef]
28. Vázquez-Calle, K.; Guillén-Mena, V.; Quesada-Molina, F. Analysis of the Embodied Energy and CO_2 Emissions of Ready-Mixed Concrete: A Case Study in Cuenca, Ecuador. *Materials* **2022**, *15*, 4896. [CrossRef]
29. Narváez, E.N.R.; Maldonado, L. Propuesta de Disminución de Huella de Carbono para Construcción de Edificaciones. Caso de Estudio: Edificio de Ciencias Básicas de la Universidad Técnica de Ambato, Ecuador. *Investig. Desarro.* **2022**, *15*, 19–31.
30. Alvarado, A.; Audin, L.; Nocquet, J.M.; Lagreulet, S.; Segovia, M.; Font, Y.; Lamarque, G.; Yepes, H.; Mothes, P.; Rolandone, F.; et al. Active tectonics in Quito, Ecuador, assessed by geomorphological studies, GPS data, and crustal seismicity. *Tectonics* **2014**, *33*, 67–83. [CrossRef]
31. Organismo Internacional de Energía Atómica. *Estudios de Hidrologia Isotopica en America Latina 2006*; IAEA: Wagram, Austria, 2009.
32. Secretaria de Territorio Habitat y V. *Plan de Uso y Gestion del Suelo*; Secretaria de Territorio Habitat y V: Quito, Ecuador, 2021.
33. Valverde, J.; Fernández, J.; Jiménez, E.; Vaca, T.; Alarcón, F. *Microzonificación Sísmica de los Suelos del Distrito Metropolitano de la Ciudad de Quito*; Escuela Politécnica Nacional: Quito, Ecuador, 2002.
34. *ASCE/SEI 7-16*; Minimum Design Loads for Buildings and Other Structures. ASCE: Reston, VA, USA, 2017.
35. Páez, D. Influencia de muros de mampostería en el comportamiento de edificios de Manta durante el terremoto de 16 de abril del 2016, Pedernales- Ecuador. In Proceedings of the Third Annual State-of-the-Art in Civil Engineering Structures and Materials Conference, Quito, Ecuador, 26–28 July 2017; pp. 1–15.
36. Ministerio de Desarrollo Urbano y Vivienda (MIDUVI). *Norma Ecuatoriana de la Construcción: Estructuras de Hormigón Armado*; Ministerio de Desarrollo Urbano y Vivienda (MIDUVI): Quito, Ecuador, 2015.
37. Ministerio de Desarrollo Urbano y Vivienda (MIDUVI). *Norma Ecuatoriana de la Construcción: Peligro Sísmico, Diseño Sismo Resistente*; Ministerio de Desarrollo Urbano y Vivienda (MIDUVI): Quito, Ecuador, 2015.
38. ACI Committee 318. *Building Requirements for Structural Concrete and Commentary*; American Concrete Institute (ACI): Farmington Hills, MI, USA, 2019; Volume 1.

39. *PAS 2050*; Specification for the Assessment of the Life Cycle Greenhouse Gas Emissions of Goods and Services. British Standards Institution: London, UK, 2011.
40. Cal, A. El Ciclo de Vida de la Madera en la Construcción. Análisis de un Caso Práctico. Master's Thesis, Universidad de la Coruña: A Coruña, Spain, 2017.
41. Hammond, G.; Jones, C. *Inventory of Carbon amd Energy (ICE)*; University of Bath—Sustainable Energy Research Team: Bath, UK, 2019.
42. Lawson, B. *Building Materials Energy and Enviroment: Towards Ecologically Sustainable Development*; The Royal Australian Institute of Architects: Manukau, New Zealand, 1996.
43. Cámara Colombiana de la Infraestructura. *Informes de Maquinaria*; Cámara Colombiana de la Infraestructura: Medellín, Colombia, 2010.
44. Andres. Potencia de Equipos Eléctricos Más Comunes. Electricaplicada. Available online: https://electricaplicada.com/potencia-consumo-equipos-electricos/ (accessed on 22 September 2022).
45. Petroecuador. *Memoria de Sostenibilidad*; Petroecuador: Quito, Ecuador, 2019.
46. Comisión Técnica de Determinación de Factores de Emisión de Gases de Efecto Ivernadero—CTFE. *Factor De Emisión De Co2 Del Sistema Nacional Interconectado De Ecuador*; Informe: Quito, Ecuador, 2019; Volume 2019.
47. Seo, M.S.; Kim, T.; Hong, G.; Kim, H. On-Site Measurements of CO2 Emissions during the Construction Phase of a Building Complex. *Energies* **2016**, *9*, 599. [CrossRef]
48. Suzuki, M.; Oka, T.; Okada, K. The estimation of energy consumption and CO_2 emission due to housing construction in Japan. *Energy Build.* **1995**, *22*, 165–169. [CrossRef]
49. Berrón Ferrer, G. Importancia de incorporar conceptos ambientales en el diseño y construcción de obras civiles. *Artíc. Divulg. Berrón G Ing.* **2003**, *7*, 52.
50. Domínguez, R.; León, M.; Samaniego, J.; Sunkel, O.; Sánchez, J. *Desarrollo Sostenible Recursos Naturales, Medio Ambiente y Sostenibilidad 70 Años de Pensamiento de la CEPAL.*; Comisión Económica para América Latina y el Caribe: Santiago, Chile, 1948.
51. Resch, E.; Lausselet, C.; Brattebø, H.; Andresen, I. An analytical method for evaluating and visualizing embodied carbon emissions of buildings. *Build. Environ.* **2020**, *168*, 106476. [CrossRef]
52. CAMICON; Ministerio de Desarrollo Urbano y Vivienda (MIDUVI). *Norma Ecuatoriana de la Construcción—NEC: NEC-SE-MP—Mamposteria Estructural*; CAMICON: Quito, Ecuador; Ministerio de Desarrollo Urbano y Vivienda (MIDUVI): Quito, Ecuador, 2014.
53. Mercimek, Ö. Seismic failure modes of masonry structures exposed to Kahramanmaraş earthquakes (Mw 7.7 and 7.6) on February 6, 2023. *Eng. Fail. Anal.* **2023**, *151*, 107422. [CrossRef]
54. Nayak, S.; Dutta, S.C. Failure of masonry structures in earthquake: A few simple cost effective techniques as possible solutions. *Eng. Struct.* **2016**, *106*, 53–67. [CrossRef]
55. Kua, H.W.; Wong, C.L. Analysing the life cycle greenhouse gas emission and energy consumption of a multi-storied commercial building in Singapore from an extended system boundary perspective. *Energy Build.* **2012**, *51*, 6–14. [CrossRef]
56. Pavlović, A.; Donchev, T.; Petkova, D.; Staletović, N. Sustainability of alternative reinforcement for concrete structures: Life cycle assessment of basalt FRP bars. *Constr. Build. Mater.* **2022**, *334*, 127424. [CrossRef]
57. Medina Romero, L. *Análisis de la Viabilidad Económica y Ambiental del uso de Armaduras Corrugadas de Acero Inoxidable en Elementos de Hormigón Armado Sometidos a Clases de Exposición Agresivas. Aplicación a Elementos en Contacto con Aguas Residuales Agresivas*; Universidad Politécnica de Cataluña: Barcelona, Spain, 2006.

Disclaimer/Publisher's Note: The statements, opinions and data contained in all publications are solely those of the individual author(s) and contributor(s) and not of MDPI and/or the editor(s). MDPI and/or the editor(s) disclaim responsibility for any injury to people or property resulting from any ideas, methods, instructions or products referred to in the content.